Research in Astron. Astrophys. **2011** Vol. **11** No. **12**, 1449–1456
http://www.raa-journal.org *http://www.iop.org/journals/raa*

***R**esearch in*
***A**stronomy and*
***A**strophysics*

The nature of orbits in a prolate elliptical galaxy model with a bulge and a dense nucleus

Nicolaos D. Caranicolas and Euaggelos E. Zotos

Department of Physics, Section of Astrophysics, Astronomy and Mechanics, Aristotle University of Thessaloniki 541 24, Thessaloniki, Greece; *caranic@astro.auth.gr, evzotos@astro.auth.gr*

Received 2011 June 3; accepted 2011 August 1

Abstract We study the transition from regular to chaotic motion in a prolate elliptical galaxy dynamical model with a bulge and a dense nucleus. Our numerical investigation shows that stars with angular momentum L_z less than or equal to a critical value L_{zc}, moving near the galactic plane, are scattered to higher z, when reaching the central region of the galaxy, thus displaying chaotic motion. An inverse square law relationship was found to exist between the radius of the bulge and the critical value L_{zc} of the angular momentum. On the other hand, a linear relationship exists between the mass of the nucleus and L_{zc}. The numerically obtained results are explained using theoretical arguments. Our study shows that there are connections between regular or chaotic motion and the physical parameters of the system, such as the star's angular momentum and mass, the scale length of the nucleus and the radius of the bulge. The results are compared with the outcomes of previous work.

Key words: galaxies: kinematics and dynamics

1 INTRODUCTION

Today astronomers believe that the intrinsic shapes of most elliptical galaxies are either oblate or prolate. It is also true that spherical galaxies are very rare but triaxial elliptical galaxies do exist (see Statler 1994; Ryden 1996; Alam & Ryden 2002; Vincent & Ryden 2005). On the other hand, there are observational data indicating the presence of a black hole or a dense massive nucleus in the central parts of elliptical galaxies (Statler et al. 2004).

All of the above gives us the opportunity to construct a dynamical model for an elliptical galaxy hosting a dense nucleus, in order to use it for the study of the global properties of motion in these stellar systems. In order to describe the motion in a prolate elliptical galaxy we use the potential

$$V_{\rm t} = \frac{\upsilon_0^2}{2}\ln\left(r^2+\alpha z^2+c_{\rm b}^2\right) - \frac{M_{\rm n}}{\sqrt{r^2+z^2+c_{\rm n}^2}} = V_{\rm g}+V_{\rm n}. \quad (1)$$

Our model consists of two components. The first component describes a prolate elliptical galaxy while the second is the potential of a dense spherical nucleus. Here r, z are the usual cylindrical coordinates, υ_0 is used for consistency of galactic units, $0.2 \leq \alpha < 1$ is the flattening parameter, and $c_{\rm b}$ is the radius of the bulge component. Furthermore, $M_{\rm n}$ is the mass and $c_{\rm n}$ is the scale length of the nucleus.

In an earlier paper (Caranicolas & Innanen 1991, hereafter Paper I) we have studied the transition from regular to chaotic motion in a disk galaxy model with a dense nucleus. There we found that stars, moving in the $r-z$ plane with values of angular momentum L_z less than or equal to a critical value L_{zc}, are scattered to higher z upon encountering the dense nucleus, thus displaying chaotic motion. We also found relationships connecting the physical parameters of the system with chaos. In the present paper, we shall focus our study on the transition from regular to chaotic motion in model (1), which describes a prolate elliptical galaxy hosting a dense nucleus. Our aim is: (i) to look for relationships between the physical parameters and chaos, (ii) to explain the numerically found relationships using a semi-theoretical approach and (iii) to compare the present results with the outcomes found in Paper I.

In this research we use the well known system of galactic units, where the unit of length is 1 kpc, the unit of mass is $2.325 \times 10^7\, M_{\odot}$ and the unit of time is 0.97748×10^8 yr. The velocity and the angular velocity units are 10 km s^{-1} and 100 km s^{-1} kpc^{-1} respectively, while G is equal to unity. The energy unit (per unit mass) is 100 km^2 s^{-2}. In the above units we use the values: $\upsilon_0 = 10$ while $0 \leq M_{\rm n} \leq 150$, $0.75 \leq c_{\rm b} \leq 1.25$ and $0.1 \leq c_{\rm n} \leq 0.25$. Since the total potential $V_{\rm t} = V_{\rm t}(r,z)$ is axially symmetric and the L_z component of the angular momentum is conserved, we use the effective potential

$$V_{\rm eff} = \frac{L_z^2}{2r^2} + V_{\rm t}(r,z)\,, \tag{2}$$

in order to study the motion in the meridian $(r-z)$ plane. The equations of motion are

$$\dot{r} = p_r, \quad \dot{z} = p_z,$$
$$\dot{p_r} = -\frac{\partial V_{\rm eff}}{\partial r}, \quad \dot{p_z} = -\frac{\partial V_{\rm eff}}{\partial z}, \tag{3}$$

and the corresponding Hamiltonian is written as

$$H = \frac{1}{2}\left(p_r^2 + p_z^2\right) + V_{\rm eff}(r,z) = E, \tag{4}$$

where p_r and p_z are the momenta per unit mass conjugate to r and z respectively, while E is the numerical value of the Hamiltonian. Equation (4) is an integral of motion, which indicates that the total energy of the particle is conserved. Orbit calculations are based on the numerical integration of the equations of motion (3), which were made using a Bulirsh-Stöer routine, to double precision. The accuracy of the calculations was checked by the constancy of the energy integral, which was conserved up to the twelfth significant figure.

The paper is organized as follows. In Section 2 we present numerical results for the potential of a non-active galaxy, that is when $M_{\rm n} = 0$. Furthermore, the numerical relationship is explained using some semi-theoretical arguments. In Section 3, we investigate numerically the case when the dense nucleus is present. Some semi-theoretical arguments are also presented, in order to explain the numerical outcomes. In Section 4 a comparison with earlier work is given and discussion and conclusions of this research are presented.

2 RESULTS WHEN THE MASSIVE DENSE NUCLEUS IS NOT PRESENT

In this Section we shall study the behavior of orbits when the dense massive nucleus is not present, that is when $M_{\rm n} = 0$. Figure 1 shows the numerical relationship between the critical value L_{zc} of the angular momentum and the radius of the bulge $c_{\rm b}$. Orbits were started near $r_0 = r_{\max}$, with $z_0 = p_{r0} = 0$, while the value of p_{z0} is always found from the energy integral (4). The value of $r_{\max}$ is the maximal root of equation

$$\frac{L_z^2}{2r^2} + \frac{1}{2}\ln\left(r^2 + c_{\rm b}^2\right) = E, \tag{5}$$

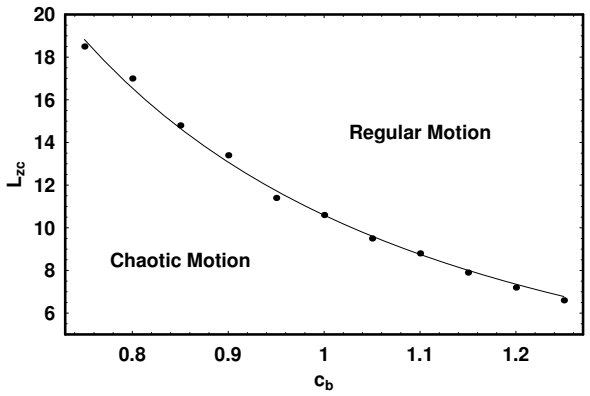

Fig. 1 Plot of L_{zc} vs. $c_{\rm b}$. The values of the parameters are given in the text.

which was found numerically. Dots represent the numerical values while the solid line is the best fit which is an inverse square law, represented by the equation

$$L_{zc} = \frac{10.5906}{c_{\rm b}^2}. \tag{6}$$

The value of α is 0.2, while the value of E is 231. Orbits with values of the parameters on and below the line are chaotic, while orbits on the upper side of the line are regular.

Figure 2 shows the Poincaré $r-p_r, z=0, p_z>0$ phase plane when $\alpha=0.2, L_z=1, E=213$, while the value of c_b is 0.75 in Figure 2(a) and 1.25 in Figure 2(b). As one can see, the pattern is similar in both figures with regions of regular and chaotic motion. A more detailed inspection shows that the extent of the chaotic zone is larger in the case when $c_b=0.75$, which is when we have a galaxy with a denser bulge. Figure 3 shows two orbits when $\alpha=0.2, c_b=0.9, E=231$. The value of the angular momentum in the orbit shown in Figure 3(a) is $L_z=40$ and the initial conditions are: $r_0=9.1, z_0=p_{r0}=0$, while the value of p_{z0} is always found from the energy integral (4). Note that the orbit is regular and stays very close to the galactic plane. On the contrary, the orbit shown in Figure 3(b) has a value of $L_z=8$ and initial conditions: $r_0=10.0, z_0=p_{r0}=0$. The orbit is chaotic and it is scattered off the galactic plane, displaying high values of z. Both orbits were calculated for a time period of 200 time units.

Let us now begin to use semi-analytical arguments in order to explain the numerically found relationship of Figure 1. The lines of arguments are similar to those used in Paper I. As the test particle approaches very close to the center of a galaxy, there is a change in its momentum in the z direction given by the equation

$$m\Delta p_z = \langle F_z\rangle \Delta t. \tag{7}$$

Here m is the mass of the test particle, $\langle F_z\rangle$ is the total average force acting in the z direction and Δt is the duration of the encounter. Empirical evidence shows that the test particle's rise proceeds cumulatively in each case, and increases a little more with each successive pass from the center rather than with a single "violent" encounter. It is observed that the test particle gains considerable height after $n(n>1)$ crossings, when the total change in the momentum in the z direction is on the order of mv_ϕ, where v_ϕ is the tangential velocity of the test particle near the center at a distance $r=\langle r_0\rangle \simeq \langle z_0\rangle \ll 1$. Therefore we write

$$m\sum_{i=1}^{n}\Delta p_{zi} \approx \langle F_z\rangle \sum_{i=1}^{n}\Delta t_i. \tag{8}$$

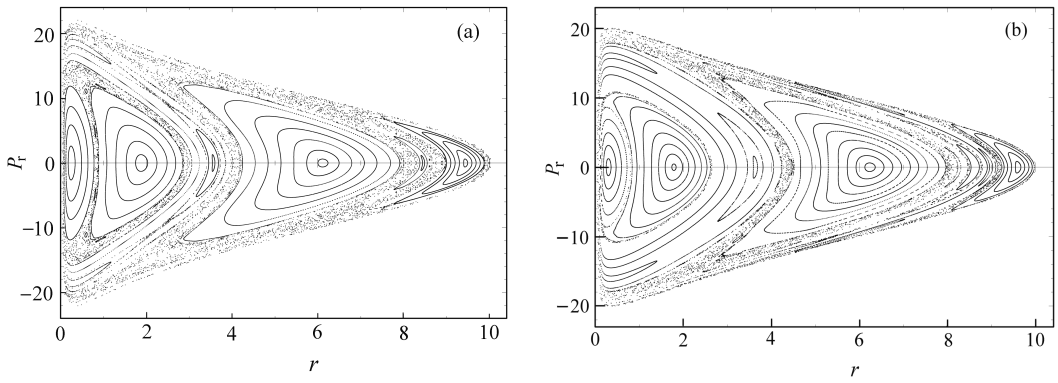

Fig. 2 $r - p_r$ phase plane when the dense nucleus is absent. (a) $c_{\rm b} = 0.75$ and (b) $c_{\rm b} = 1.25$. The values of all other parameters are given in the text.

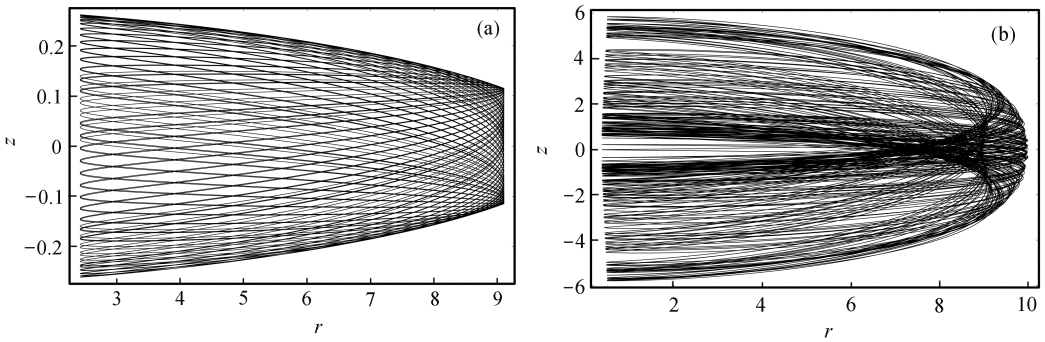

Fig. 3 Orbits when the dense nucleus is not present. (a) A regular orbit which stays near the galactic plane. (b) A chaotic orbit which is scattered into high values of z. See the text for details.

Setting

$$m\sum_{i=1}^{n}\Delta p_{zi} \;=\; mv_{\phi} = \frac{mL_{zc}}{\langle r_0\rangle}\,,$$
$$\sum_{i=1}^{n}\Delta t_i \;=\; T_c, \tag{9}$$

in Equation (8) we find

$$\frac{mL_{zc}}{\langle r_0\rangle} \;\approx\; \langle F_z\rangle T_c. \tag{10}$$

The force acting in the z direction for a test particle of unit mass $(m = 1)$ is

$$F_z = \frac{-v_0^2\alpha z}{r^2 + \alpha z^2 + c_{\rm b}^2}. \tag{11}$$

Remember that $r = \langle r_0\rangle \simeq \langle z_0\rangle \ll 1$, therefore $\langle r_0^2\rangle \simeq \langle z_0^2\rangle \ll c_{\rm b}^2$. Keeping only the linear terms in $\langle r\rangle$ and $\langle z\rangle$ in Equation (11) and taking the absolute value of the F_z force, we find from relationship

(10) that

$$L_{zc} \approx \frac{v_0^2 \alpha (\langle r_0 \rangle)^2}{c_{\rm b}^2} T_c. \tag{12}$$

Since T_c was observed to be the same when $0.75 \leq c_{\rm b} \leq 1.25$, we can set $k_1 = v_0^2 \alpha \left(\langle r_0 \rangle\right)^2 T_c$ and obtain

$$L_{zc} \approx \frac{k_1}{c_{\rm b}^2}, \tag{13}$$

which explains the numerical relationship of Figure 1. The authors would like to make it clear that relation (13) does not reproduce the numerical results shown in Figure 1, but only shows the form of the relationship.

3 RESULTS WHEN THE MASSIVE NUCLEUS IS PRESENT

We investigate the case when we have an active galaxy, that is when the dense massive nucleus is present. Figure 4 shows a numerical relationship between the critical value L_{zc} of the angular momentum and the mass of the nucleus $M_{\rm n}$ for two values of $c_{\rm n}$. The procedure to obtain the results shown in Figure 4 is similar to that followed in Figure 1. The value of α is 0.5, $c_{\rm b} = 1.2$, while the value of E is 227. Here we see a straight line. Orbits with values of the parameters on the left side of the line, including the line, are chaotic, while orbits on the right side of the line are regular. It is interesting to note that the extent of the chaotic region is larger when the value of $c_{\rm n}$ is smaller, which is when we have a denser nucleus.

Figure 5(a)–(b) shows the Poincaré $r - p_r, z = 0, p_z > 0$ phase plane when: $\alpha = 0.2, L_z = 10, E = 230, c_{\rm b} = 1.2$; the value of $M_{\rm n}$ is 20 in Figure 5(a) and 100 in Figure 5(b). In both cases, we observe regular regions together with large chaotic regions. Some small islands are also present indicating secondary resonances. It is evident that the area covered by chaotic orbits is larger in the case of $M_{\rm n} = 100$, which is when we have a more massive nucleus. In Figure 6(a)–(b) we can see two orbits when $\alpha = 0.5, c_{\rm b} = 1.2, E = 227$. The value of the angular momentum in the orbit shown in Figure 6(a) is $L_z = 60$, while the value of $M_{\rm n}$ is 25 and $c_{\rm n} = 0.25$. The initial conditions are $r_0 = 6.0, z_0 = p_{r0} = 0$, while the value of p_{z0} is always found from the energy integral (4). Note that the orbit is regular, and stays very close to the galactic plane. On the other hand, the orbit shown in Figure 6(b) has a value of $L_z = 45$, while the value of $M_{\rm n}$ is 120 and $c_{\rm n} = 0.25$. Initial conditions are: $r_0 = 9.768, z_0 = p_{r0} = 0$. The orbit is chaotic and it is scattered off the galactic plane, displaying high values of z. Both orbits were calculated for a time period of 200 time units.

The linear relationship of Figure 4 can be obtained using semi-analytical arguments. As the test particle approaches the nucleus it experiences a strong vertical force, due to the presence of the dense nucleus.

Figure 7 shows a plot of the F_z force as well as the nuclear F_{zn} force as a function of z, near the nucleus when $r_0 = 0.1$. The values of the parameters are $\alpha = 0.5, v_0 = 10, c_{\rm b} = 0.8, M_{\rm n} = 100, c_{\rm n} = 0.25$. We see that the nuclear force is about 25 times as strong as F_z. Because of this strong force, there is a change in its momentum in the z direction given by the equation

$$m \Delta p_z = \langle F_{zn} \rangle \Delta t, \tag{14}$$

where m is the mass of the test particle, $\langle F_{zn} \rangle$ is the average nuclear force acting in the z direction, while Δt is the duration of the encounter. Here again, our numerical results show that the test particle goes to higher z after $n (n > 1)$ crossings, when the total change in the momentum in the z direction is on the order of $m v_\phi$, where v_ϕ is the tangential velocity of the test particle near the center, at a distance $r_0 \simeq z_0 \simeq c_{\rm n}$. Therefore we write

$$m \sum_{i=1}^{n} \Delta p_{zi} \approx \langle F_{zn} \rangle \sum_{i=1}^{n} \Delta t_i. \tag{15}$$

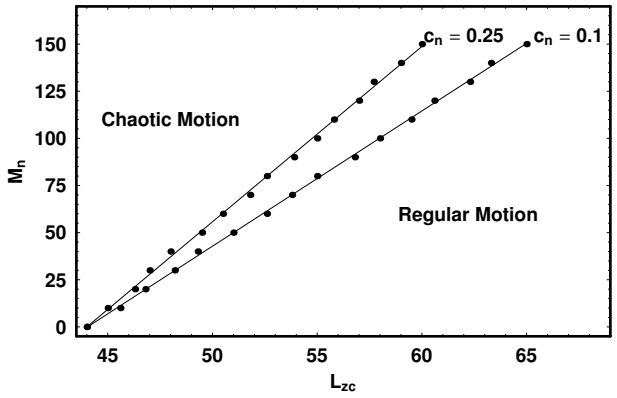

Fig. 4 Plot of $M_{\rm n}$ vs. L_{zc}. The values of the parameters are given in the text.

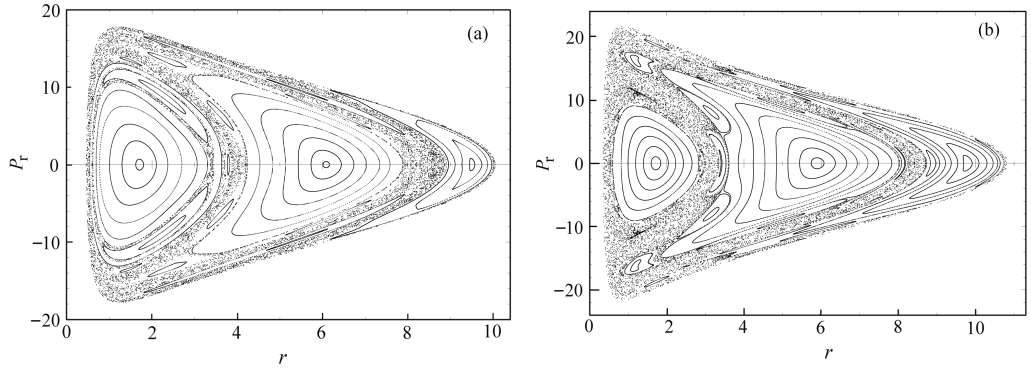

Fig. 5 $r - p_r$ phase plane when the dense nucleus is present. (a) $M_{\rm n} = 20$ and (b) $M_{\rm n} = 100$. The values of all other parameters are given in the text.

If we set

$$\begin{aligned} m\sum_{i=1}^{n}\Delta p_{zi} &= m v_\phi = \frac{mL_{zc}}{\langle r_0\rangle}, \\ \sum_{i=1}^{n}\Delta t_i &= T_e, \\ m &= 1, \\ \langle F_{zn}\rangle &= \frac{c_{\rm n}M_{\rm n}}{(3c_{\rm n}^2)^{3/2}}, \end{aligned} \tag{16}$$

in Equation (15) we obtain

$$M_{\rm n} \approx k_2 L_{zc} c_{\rm n}, \tag{17}$$

where $k_2 = \sqrt{27}/T_e$. Note that the values of T_e were observed to be about the same when $0 < M_n \leq 150$. Equation (17) explains the numerically found relationship given in Figure 4.

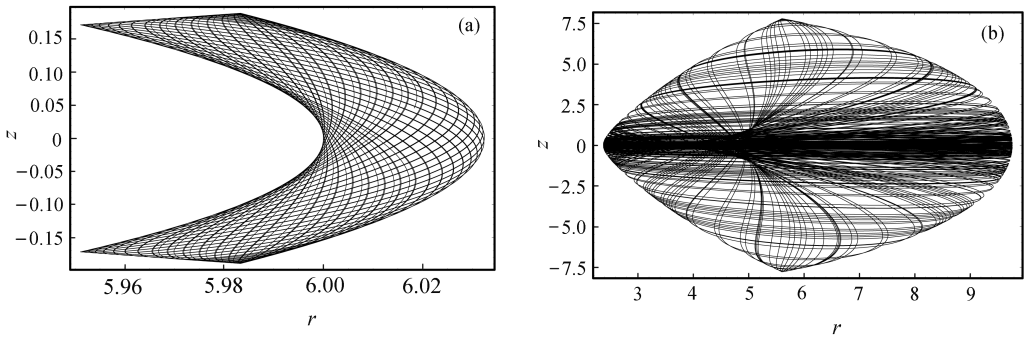

Fig. 6 Orbits when the dense nucleus is present. (a) A regular orbit which stays near the galactic plane. (b) A chaotic orbit which is scattered into high values of z. See the text for details.

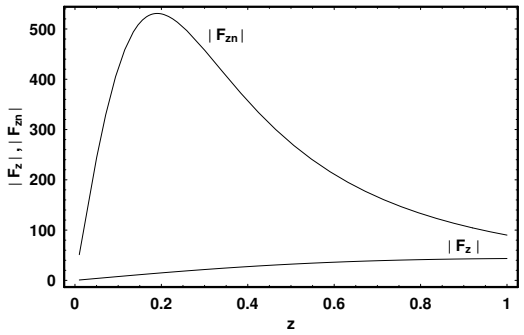

Fig. 7 Plot of $|F_z|$ and $|F_{zn}|$ vs. z. The values of all the other parameters are given in the text.

4 DISCUSSION

Today it is well-known that there are luminous elliptical galaxies hosting dense massive nuclei (see Urry et al. 2000). During the past few years, a large amount of observational data has given a better and more detailed picture of these active galaxies (Barth et al. 2002; Costamante & Ghisellini 2002; Falomo et al. 2002; Vagnetti et al. 2003; Falcone et al. 2004; Heidt et al. 2004; Bramel et al. 2005; Nieppola et al. 2006; Zheng et al. 2007).

In this article we have studied the transition from regular to chaotic motion in a prolate elliptical galaxy model. Two cases were studied, which are the case where the nucleus was absent and the case where we have an active galaxy hosting a dense massive nucleus. In the first case we found that an inverse square law relationship exists between the radius of the bulge of the galaxy and the critical angular momentum when all other parameters are kept fixed. This relationship was also reproduced, using some semi-analytical arguments.

On the other hand, it was observed that for larger values of the radius of the bulge, for $c_{\rm b} \geq 1.5$, the chaotic regions when the dense nucleus is absent, if any, are negligible when $0.2 \leq \alpha < 1$. This result is in agreement with the result found in Paper I, where no chaos was observed when $c_{\rm b} > 1.3$ and this result was independent of the mass of the bulge. Thus, our results suggest that chaos is observed in disk and prolate elliptical galaxies when a dense bulge is present.

Interesting results are obtained when a dense nucleus is present. In this case the numerically found relationship connecting L_{zc} and $M_{\rm n}$ is linear when all other parameters are kept constant.

Furthermore, the linear relationship depends on the value of $c_{\rm n}$, in such a way that the extent of the chaotic region is larger when $c_{\rm n}$ is smaller, which is when the nucleus has a higher density. The linear relationship obtained by the numerical integration of the equations of motion was also found using some semi-theoretical arguments, together with numerical evidence.

The present investigation shows that the results obtained are very similar to those obtained for disk galaxies in Paper I. Therefore, we can say that low angular momentum stars approaching a dense massive nucleus are deflected to higher z, thus displaying chaotic motion. The similarity of the results obtained for different galactic models suggests that it is the strong vertical force near the dense nucleus that is responsible for this scattering combined with the star's low angular momentum, which allows the star to approach the dense nucleus.

Some of the latest discoveries obtained from observational astronomy show that supermassive black holes, up to a billion solar masses, inhabit the centers of all massive spheroidal galaxies, independent of their visible activity; the supermassive black holes are often quiescent with regard to their own radiation but always show dynamical behavior. We believe that, with new data from active galaxies, astronomers will be able to construct better dynamical models in the near future, in order to study the properties of motion in galaxies and to find interesting relationships connecting chaos with the physical parameters of these stellar systems.

Acknowledgements Useful suggestions and comments from an anonymous referee are gratefully acknowledged.

References

Alam, S. M. K., & Ryden, B. S. 2002, ApJ, 570, 610
Barth, A. J., Ho, L. C., & Sargent, W. L. W. 2002, ApJ, 566, L13
Bramel, D. A., Carson, J., Covault, C. E., et al. 2005, ApJ, 629, 108
Caranicolas, N. D., & Innanen, K. A. 1991, AJ, 102, 1343 (Paper I)
Costamante, L., & Ghisellini, G. 2002, A&A, 384, 56
Falcone, A. D., Cui, W., & Finley, J. P. 2004, ApJ, 601, 165
Falomo, R., Kotilainen, J. K., & Treves, A. 2002, ApJ, 569, L35
Heidt, J., Tröller, M., Nilsson, K., et al. 2004, in The Interplay Among Black Holes, Stars and ISM in Galactic Nuclei, IAU Symposium 222, eds. T. Storchi-Bergmann, L. C. Ho, & H. R. Schmitt, 521
Nieppola, E., Tornikoski, M., & Valtaoja, E. 2006, A&A, 445, 441
Ryden, B. S. 1996, ApJ, 461, 146
Statler, T. S. 1994, ApJ, 425, 500
Statler, T. S., Emsellem, E., Peletier, R. F., & Bacon, R. 2004, MNRAS, 353, 1
Urry, C. M., Scarpa, R., O'Dowd, M., et al. 2000, ApJ, 532, 816
Vagnetti, F., Trevese, D., & Nesci, R. 2003, ApJ, 590, 123
Vincent, R. A., & Ryden, B. S. 2005, ApJ, 623, 137
Zheng, Y. G., Zhang, X., & Bi, X. W. 2007, PASP, 119, 477